Thermal Stratification in the Air Basin over the Moscow Metropolis: Comparison of Model and Observational Data

V. P. Yushkov*

Moscow State University, Moscow, 119991 Russia
***e-mail: yushkov@phys.msu.ru**

Abstract—Data obtained from long-term systematic measurements of thermal stratification in the atmospheric boundary layer (ABL) over the Moscow metropolis and simulation data obtained using a high-resolution mesoscale model have been compared. Model results demonstrate there to be a more stable stratification (when compared to observational data) at night in winter. Under conditions of unstable stratification, even in winter, models dampen inhomogeneities that take place too rapidly, which leads to an underestimation of the spectrum of mesoscale fluctuations, average gradients, and their dynamics in the lower part of the ABL in the models. A simple algorithm for estimating errors in numerical forecasts is proposed and it is shown that errors in near-surface temperature forecasts are mainly associated with the simulation of processes occurring in the ABL. It is also shown that microwave radiometers operating within a band of 60 GHz may be a simple and reliable tool for estimating the accuracy of boundary-layer parameterizations in numerical weather-forecast models.

INTRODUCTION

In recent decades, hydrodynamic weather-forecast models, such as WRF [1], COSMO [2], ICON [3], and many others, have become accessible for a wider range of studies, and more specialists have had the opportunity to compare model results with remote sensing data. Such models become more and more detailed, they allow for a lot of parameterizations of both microphysical and turbulent processes. Therefore, the advent of new measurement methods has provided new possibilities to solve the problem of the accuracy and efficiency of detailed weather forecasts: it has become possible to estimate the accuracy in simulating not only the field of pressure or geopotential but also thermal stratification in the atmospheric boundary layer (ABL), the intensity of turbulent mixing, or, for example, the humidity content of clouds and the distribution of drops and crystals in them [4–6].

With increased urban population, city area and changes in the character of housing development in large cities, the question of the ability of modern high-resolution hydrodynamic models to adequately describe the impact of human beings on the environment becomes urgent. It is well known that the ABL thermal stratification determines mixing within this layer [7, 8] and affects the concentration of atmospheric pollutants in large metropolises [9]. In addition, an adequate simulation of thermal stratification in the ABL, in its lower part and right by the surface in numerical models and allowance for the mesoscale inhomogeneities of underlying surface properties lead to the improvement of models and our understanding of turbulent mixing processes.

In this work, data obtained from long-term remote sensing of vertical temperature profiles in the ABL using a scanning microwave radiometer (MTP-5) have been compared with model calculations using detailed mesoscale atmospheric circulation model (WRF-ARW). Such an analysis may be recommended for other models, parameterization schemes, or other methods of retrieving temperature profiles based on remote sensing.

1. URBAN HEAT ISLAND AND TEMPERATURE MEASUREMENS IN THE ATMOSPHERIC BOUNDARY LAYER

The impact of human activities on the environment is diverse, and the temperature field is only the simplest indicator of such an impact. Reliable measurements of even slight temperature-field variations make it possible to test hydrodynamic models of atmospheric processes and estimate the reliability of transport models, which is important, for example, in calculating pollutant concentrations. At the same time, the ABL thermal stratification determines turbulent mixing characteristics and the vertical fluxes of heat, momentum, humidity, and gaseous pollutants.

A large body of measurement data obtained over both urban and rural areas [10−12] demonstrate a characteristic pattern of temperature-field variations, which depends on the geographic position of a metropolis, season, day, and height above ground level (AGL). For example, it is known that the urban heat island (UHI) according to measurement data obtained at meteorological stations and the surface IR radiation field (SUHI) according to satellite measurements significantly differ in diurnal variation and intensity [13−15], and, under conditions of an arid climate, the vegetation of urban settlements results in the formation of even cold islands [16]. However, satellite observations do not allow one to measure the vertical extent of an island of heat or cold and estimate the influence of a city on the whole air basin, and, in numerical models, the vertical extent of heat islands depends on parameterizations. Using data obtained from a regular ground-based remote sensing, one can determine to what extent models can adequately describe the urban ABL.

Remote-sensing measurements at heights of hundreds of meters AGL require special instruments. Microwave radiometry of the ABL, the principles and methods of which were formulated already in the middle of the last century [17], has become a reliable tool for such regular measurements [18−20]. Other methods, such as aerological sounding and measurements from high-rise towers using autonomous flying vehicles, have a wide range of problems: infrequent measurements within the diurnal cycle, challenging mounting, the influence of the tower body on in situ temperature measurements, complicated and expensive continuous monitoring when organizing the take-off and landing of drones, etc.

Although radiometric measurements also have systematic errors in retrieving temperature profiles, these errors may be reduced significantly in estimating average thermal stratification, i.e., the vertical air-temperature difference. The fundamental limitation of the accuracy of measurements with a scanning radiometer is the use of the approximation of a horizontally homogeneous temperature field and its stationarity on the measurement scale. Therefore, spatial or fast turbulent variations in the temperature field lead to errors in retrieving its vertical profile. These errors are evident when a comparison is made with in situ measurements using captive balloons or flying vehicles. The method of mounting the monitor temperature sensor of the microwave radiometer yields one more significant error that depends on measurement methods, the instrument location, and synoptical conditions [21].

The characteristic general measurement error may be estimated by comparing vertical T_z and horizontal T_x temperature gradients. If the limit of accuracy for a temperature profiler may be estimated as 1°C/km, the synoptical inhomogeneity of T_x is on the order of 1°C/100 km (see Fig. 2), i.e., is two orders of magnitude lower. At the same time, this instrument is incapable of measuring and retrieving the spatial temperature inhomogeneities with scale $T_x = 1$°C/km, which are quite possible and observed in the urban environment and require a special, more complicated measurement method. In other words, a temperature microwave profiler is a high-technology and reliable tool for measuring the ABL thermal stratification on time scales of 10−15 min, which is averaged over a spatial scale of a few kilometers, without either high-frequency or spatial variations. However, numerical synoptical models do not entail a description of such variations either.

Although microwave radiometry yields reliable measurement data on the ABL average thermal stratification, it does not allow predicting its changes and does not give a spatial pattern of the temperature field over the metropolis, whose changes are associated with synoptical conditions, wind velocity, and wind direction. The question of whether numerical models can adequately describe the temperature stratification field over the city will be discussed in this work.

2. A HIGH SPATIAL RESOLUTION NUMERICAL MODEL AND POINTS FOR MEASURING TEMPERATURE PROFILES

For already several years, in parallel with the remote measurements of thermal stratification, calculations using a WRF regional mesoscale model with a horizontal resolution of 2 km and increased number of vertical levels in the ABL have been carried out at the Department of Physics of Moscow State University (MSU) in cooperation with the Russian Hydrometeorological Research Center [22]. The WRF model with an AWR dynamic core (versions 3.8 and 3.9) was used to carry out this investigation [23, 24]. Results obtained from calculations using the GFS global forecast model [25] with a spatial resolution of 0.5° were used as both initial and boundary conditions. To obtain a high spatial resolution, the model calculations were performed on three nested grids (18, 6, and 2 km) with a one-way transmission of boundary conditions. The Moscow metropolis was located in the center of each domain (see Fig. 2). Each grid had 100 nodes in two horizontal directions in the Lambert projection and 31 vertical levels (up to 50 hPa) with their concentration within the ABL.

The results obtained from numerical calculations with the parameterization—cloud microphysics (Thompson [26]), short- and long-wave radiation (RRTMG [27]), and a model of soil processes (Noah [28])—were used for comparison with measurement data. The convection parameterization according to the Grell scheme [29] was used for the grid with a resolution of 18 km. The Bougeault and Lacarrere scheme [30] based on solution of the turbulent kinetic energy (TKE) equation was used to describe mixing within the ABL on mesoscales. In this scheme, an antigradient term is

additionally introduced to describe the heat flux within the convective boundary layer [31]. In this scheme, the length scale is determined as a distance that an ensemble of air particles with a given TKE value can travel [30].

A separate urban layer parameterization was not used on the grids with resolutions of 18 and 6 km, and the urban-environment effect was described by specifying the underlying surface parameters at urban points (roughness, albedo, and both thermal capacity and conductivity of the soil). A single-level urban surface-layer model (SLUCM [32]) was used for the grid with a resolution of 2 km. In this model, an additional heat source—the city itself—is given and the effects of shading and reflections in urban street canyons are taken into account. The average anthropogenic heat flux was given in 20, 50, and 90 W/m^2 to suit the dominating type of buildings in each urban grid cell (low intensity, high intensity, and industrial).

The parameterizations used in the model were selected so that calculation results showed the best correlation with measurement data on temperature profiles and wind velocity in Moscow oblast [22]. The calculations may also be performed for other parameterization schemes or with changes in the calculation grid; however, this does not seem to significantly change the results of this work.

In this work, the emphasis is on the comparison of measurement data obtained at MSU, in the southwestern part of the capital, and in Zvenigorod (50 km from the city center). The observation conditions in Zvenigorod correspond to countryside conditions and may be considered reference conditions in studying the Moscow urban heat island [33]. The MTP-5 profiler is installed at the Zvenigorod Scientific Station (ZSS, 55°41′44.14″ N, 36°46′32.18″ E) of the Obukhov Institute of Atmospheric Physics (IAPh). The profiler is installed at a height of 15 m AGL. At the MSU, the profiler is installed on the roof of the building of the Physical Department (55°42′00.28″ N, 37°31′45.30″ E) at a height of 40 m AGL. Although this measurement point is located not in the center of Moscow but on the hill of Vorob'evy Gory, the temperature field over this locality is characteristic of the present-day urban environment. The MTP-5 temperature microwave profilers (with a sounding height of up to 600 m) operating in the center of the 5-mm oxygen absorption band are used in these two measurement points [34].

With the assistance of the Central Aerological Observatory (CAO) of the Federal Service for Hydrometeorology and Environmental Monitoring, the Moscow Ecological Monitoring (MEM) network, and the IAPh, the measurement data obtained at these points were compared with data obtained over the center of Moscow and its eastern outskirts. In the center of Moscow, in the Yakimanka district, the profiler is installed on the roof of the IAPh building

(55°44′20.81″ N, 37°37′23.57″ E) at a height of 13 m AGL. One more instrument is installed in the Moscow eastern outskirts (Kosino district, 55°43′3.09″ N, 37°56′13.20″ E) at a height of 4 m AGL. The profilers modified to operate on the "slope" of the emission band, i.e., with a higher sensitivity to air-temperature variations at high altitudes and a sounding height of up to 1000 m, were installed at these two points.

One more measurement point, at which the observations of vertical temperature profiles are regularly carried out, is located in the north of Moscow at the CAO (55°55′30.43″ N, 37°31′24.26″ E) at a height of 20 m AGL. These measurements have been taken for many years with participation of the developers of this instrument and checked by launching aerosondes in the immediate vicinity of the measurement point. Data obtained from these measurements, as well as from the measurements in Ostankino in the vicinity of the Ostankino TV tower (55°49′16.39″ N, 37°36′45.04″ E), were also analyzed, but they are not described in this work. The comparison of observational data obtained at all points showed that the instruments of both first and second modifications reliably monitor air-temperature field features in the urban environment, the vertical profiles demonstrate their general properties (see Fig. 7). The location of the measurement points is shown in Fig. 2.

3. MEASURED AND SIMULATED TIME SERIES AND TEMPERATURE FIELDS. ERRORS IN FORECASTING AND SIMULATING THERMAL STRATIFICATION

In this work, to study the quality of simulating the ABL thermal stratification in the models, we have chosen a small lead-time range (3−27 h) for numerical predictions. Such a limitation allows one to consider errors in forecasting current synoptical situations and those in simulating processes in the ABL to have approximately the same order (see Fig. 1). Running the model only once a day (but during many years) saves calculation resources and makes it possible to focus not on the accuracy of weather forecasts, but on the properties of model fields with a high spatial resolution under different synoptical conditions.

This quasi-continuous series of forecasts with an hourly time step may later be compared to data obtained from regular measurements of temperature, wind velocity, and turbulence time series at the observation points and, at the same time, such numerical calculations allow one to analyze the spatial pattern of model field inhomogeneities (see Fig. 2), which cannot be understood from solely local measurement results.

Spatial variability of the temperature field in model calculations allows one to state that vertical gradients (thermal stratification) or temperature differences between the ABL lower and upper parts more accu-
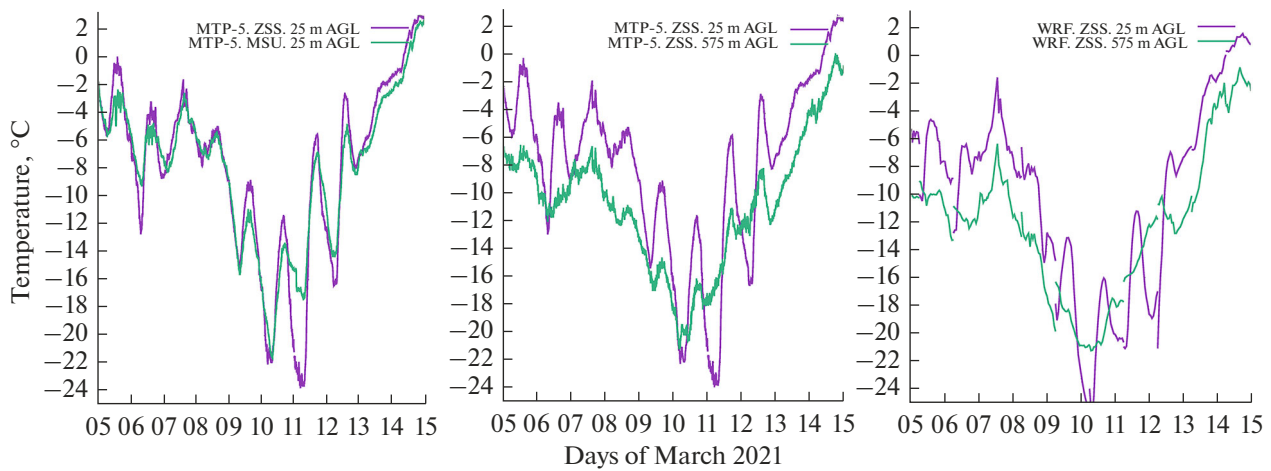
Fig. 1. Episode of temporal air-temperature variations at two points within the urban (MSU) and rural (ZSS) localities according to MTP-5 observational data and numerical (WRF) simulation in the lower (25 m) and upper (575 m) parts of the ABL. March 2021.

rately characterize the heat-island dynamics than do differences in data obtained from surface measurements at meteorological stations. This conclusion is supported by comparing data obtained from synchronous measurements of temperature profiles at the MSU and ZSS (see Fig. 1a).

Using one episode as an example, Fig. 1a shows that a significant temperature difference between urban and rural localities (a heat island) is rather rarely observed. In the absence of significant diurnal variations in radiation cooling and heating and under average turbulent mixing conditions with continuous stratus clouds within the cold season, the temperature difference between the urban and rural localities amounts to only about 1°C and reaches 6°C only in exceptional cases of strong inversions under slight cloudiness and low wind velocity (see Fig. 6). In the daytime, the near-surface heat island is almost not pronounced (see also [33]).

On the whole, it is seen in Fig. 1c that the numerical models within a small lead-time range are sufficiently successful, because, in this case, the initial conditions correspond to assimilated observational data. In addition, in Fig. 1c, the jumps in temperature between the forecasts with lead times of 3 and 27 h are a convenient measure of errors and discrepancies in numerical forecasts (see Fig. 3). At the same time, it is seen that the numerical forecast does not quite accurately simulate temperature differences between levels of 600 and 0 m: minima are reached on other days, and maxima are not so clearly pronounced as in observations. Below, we will look for the cause of these errors.

Figure 2 shows the temperature field at the instant of maximum inversion on March 11, 2021. Two features of this field are clearly seen: the heat island over Moscow in the vicinity of the surface and slight spatial temperature variations at heights of about 600 m. It is clear that the model temperature difference $T_0 - T_{600}$
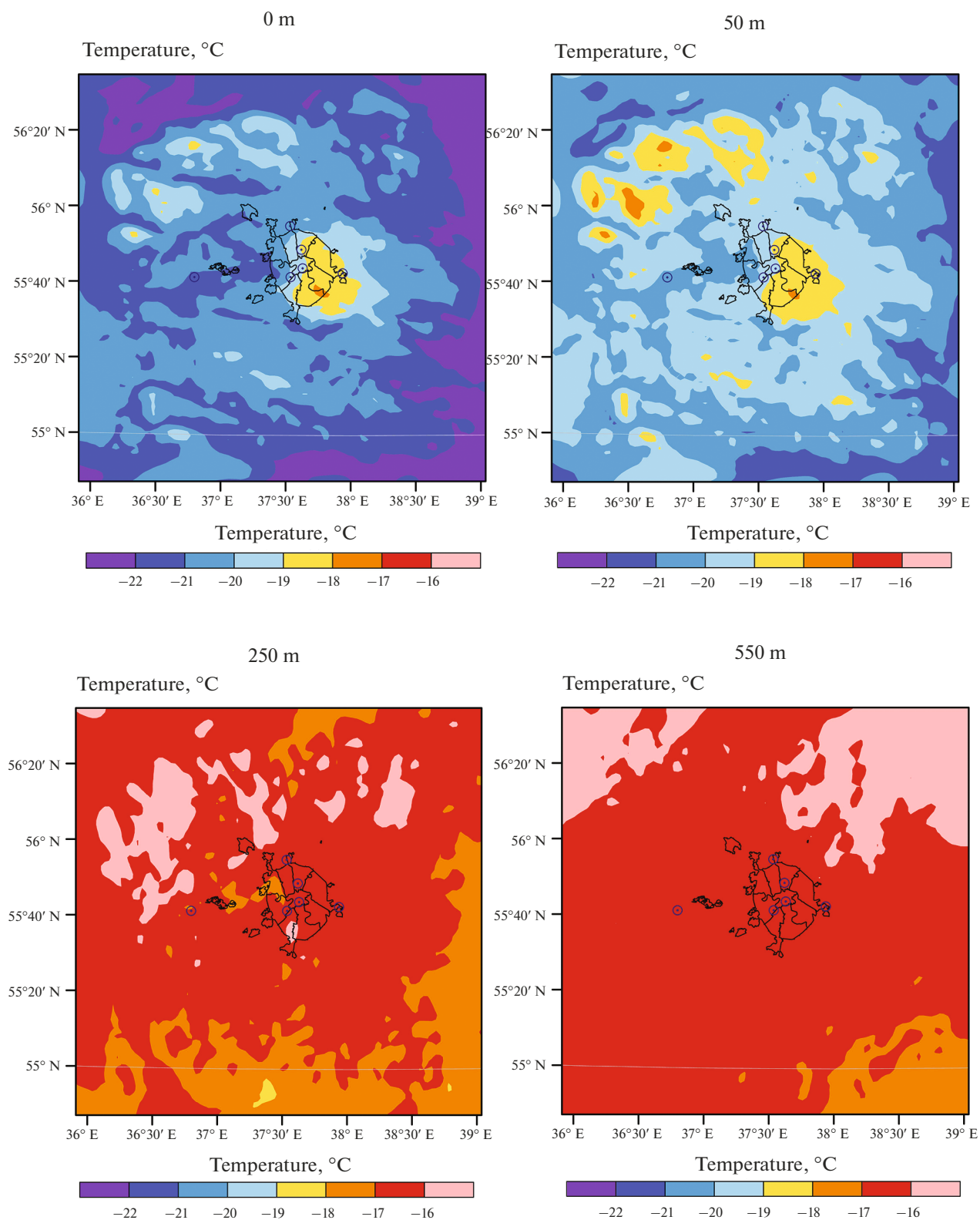
will characterize the urban heat island without regard to errors in forecasting the air-mass dynamics, and comparing this difference between model and measurement data allows one to better estimate parameterizations of turbulent mixing in the ABL in different models.

Note also that the spatial temperature field inhomogeneity (clearly seen in Fig. 2), which depends on the orography of locality and the velocity and direction of wind, statistically characterizes the anisotropic turbulence of mesoscale fluctuations and, in future, may become a source of information on turbulent mixing in the ABL.

4. FORECAST ERRORS AND THEIR RELATION TO ERRORS IN SIMULATING THE ABL

Numerical forecasts with different lead times have different accuracies. Therefore, the difference in model temperature fields between successive forecasts, for example, with lead times of 3 and 27 h contains important information on numerical model properties: having constructed the statistical distribution of this difference for different heights, different seasons, and different points, we obtain information about where the forecast errors are more significant, what their bias is (systematic error), and whether these errors are associated with the parameterization of processes in the ABL or underlying surface properties.

Statistical analysis of such errors is rather simple. This analysis shows that it is the simulation of the ABL and surface processes that mainly contributes to biased forecasts. Figure 3 shows the empirical distributions of the difference between the temperature forecasts with lead times of 3 and 27 h ($T_3 - T_{27}$) together with their approximation by the normal distribution ("fit") in such a way as to see the difference between the aver-

0 m

Temperature, °C

50 m

Temperature, °C

Temperature, °C

Temperature, °C

250 m

Temperature, °C

550 m

Temperature, °C

Temperature, °C

Temperature, °C

Fig. 2. Model air-temperature fields at different heights AGL for the strong inversion of March 11, 2021 (06:00 LST, see Fig. 1), the boundaries of the Moscow metropolis, and the points of location of the microwave profilers.
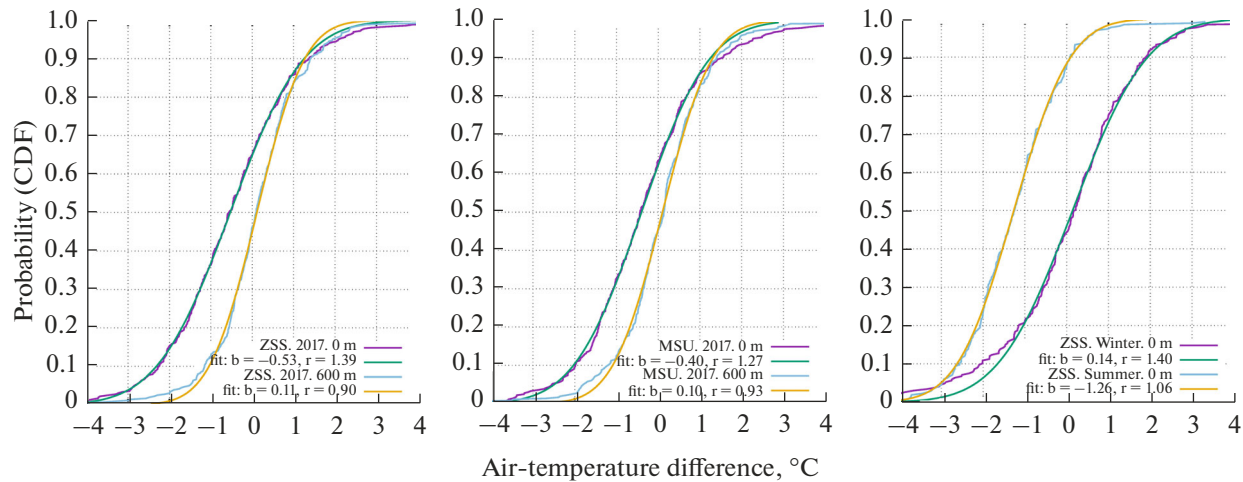
Fig. 3. Distribution of the air-temperature difference in numerical forecasts with lead times of 3 and 27 h within the surface air layer and in the upper part of the ABL for both urban (MSU) and rural (ZSS) localities in winter (DJF) and summer (JJA). The approximation by the normal distribution (fit) shows the bias (b) and rms deviation (r) of errors in degrees.

ages and variances and the adequacy of the normal distribution for these errors in most cases.

It is clearly seen that, at the level of the first model, it is the errors in forecasting surface temperature that are more biased and have a wide scatter (rms deviation). Figure 3 shows the offset (by median) and rms deviation for the approximating curves of the normal distribution. Although the difference in the model errors between the urban and rural localities is noticeable, it is not significant, which may suggest that the influence of the underlying surface on the ABL is described in insufficient detail or only slightly affects the distribution of errors. In other words, changes in the model or the boundary layer parameterization used in it may be estimated by how much this parameterization reduces the forecast bias by 24 h.

One more conclusion that follows from the analysis of such errors: the bias is more significant in summer, when the ABL stable stratification is regularly observed at night and its forecast is difficult due to errors in describing subgrid turbulent processes.

5. TEMPERATURE STRATIFICATION AT DIFFERENT HEIGHTS AND IN DIFFERENT SEASONS

Altitudinal extent and its variations are important features of a heat island. Therefore, the thermal stratification profiles are a detailed characteristic of the ABL temperature field. However, the methods of comparing measurement and simulation data may be chosen in different ways. In this work, we have restricted ourselves to the most obvious conclusions. According to data obtained from a preliminary analysis, we have chosen three height ranges that are convenient for comparison from both calculation and methodological perspectives: within the lower ABL

(0−200 m), the upper ABL (600−400 m), and throughout the whole height range (0−600 m).

In Fig. 4, to compare stratification within different height ranges, the difference between the levels is reduced to the average vertical gradient per 100 m. In this case, it is more convenient to compare this difference with a dry-adiabatic gradient and an average temperature gradient within the whole ABL. It is seen that, in summer, the interdiurnal variations in thermal stratification are wider at night. During daylight hours, the thermal stratification near the surface becomes superadiabatic with significant variations (alternation of stratification) on time scales of tens of minutes (compare with Fig. 7).

In winter, under conditions of continuous stratus clouds, the thermal stratification remains weakly stable (from 0 to 1°C/100 m) both by day and at night; moreover, in the vicinity of the surface, its heat emission is often sufficient to provide stratification that is close to neutral. On clear days with anticyclonic weather conditions, stable stratification (temperature inversion) is characteristic of the whole day and covers the entire ABL. Within the transition periods, in fall and early spring, clear cloudless days with significant diurnal radiation-balance variations clearly demonstrate the relation of the difference in thermal stratification between the urban (Fig. 5a) and rural (Fig. 4b) localities with synoptical conditions.

The practical important conclusion that follows from the analysis of Figs. 4 and 5: it is rather difficult to compare the thermal-stratification variations observed in the urban environment with their model calculations on a long time interval due to the fact that the diurnal stratification variations constantly vary in amplitude, because they depend on synoptical conditions. In addition, errors in the model description of
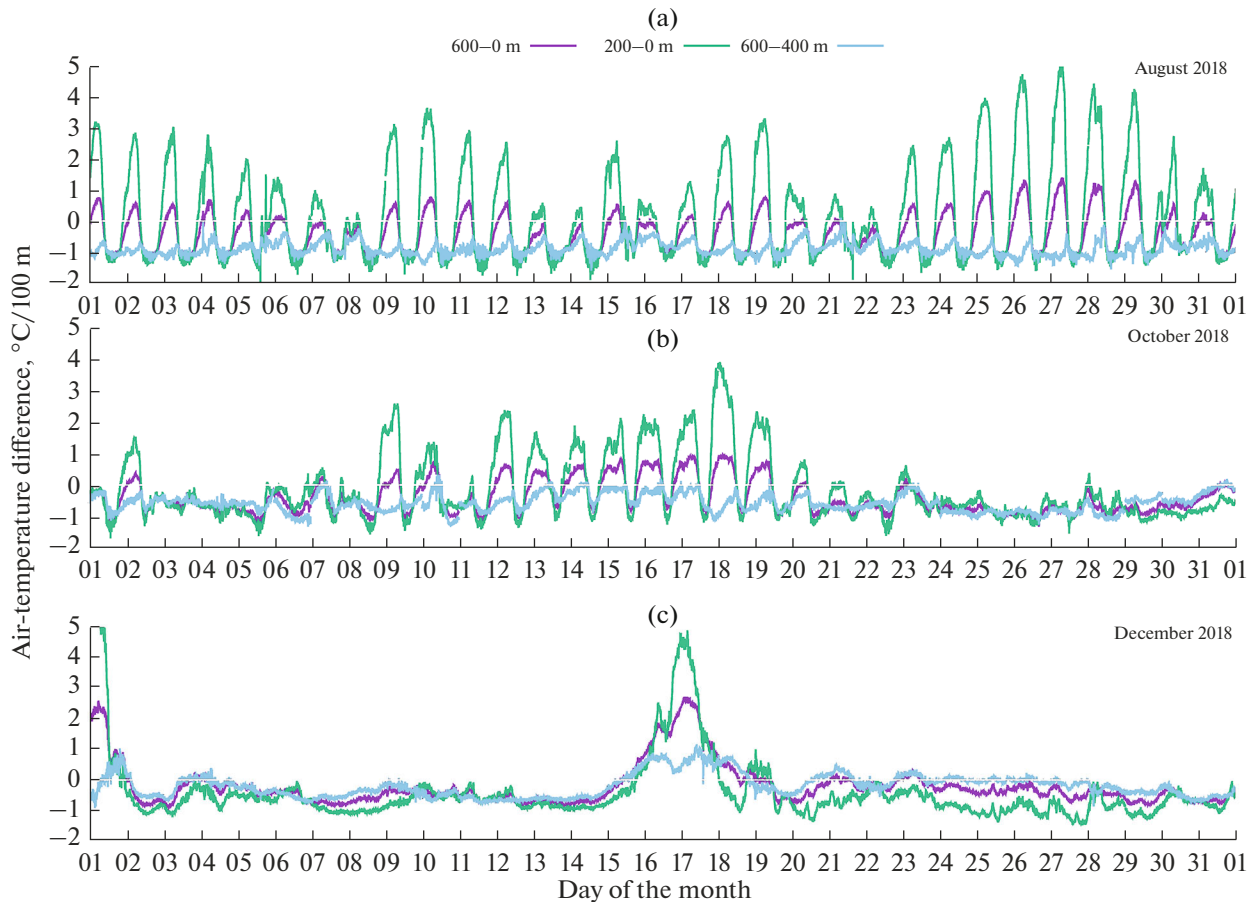
Fig. 4. The character of the diurnal variations in average air-temperature gradients within the ABL (0−600 m) for the rural locality (ZSS) and in its lower (0−200 m) and upper (400−600 m) parts (a) for summer (top), (b) fall (middle), and (c) winter (bottom).

thermal stratification will be neither a stationary random process, nor independent random variables.

Therefore, using a parameter that is similar, for example, to the Monin−Obukhov scale $L_B^{-1} = g\Delta T / T_0 U^2$ or the Richardson number $Ri_B = z/L_B = gz\Delta T / T_0 U^2$, where, for height $z = 200$ m, U is the wind velocity at this height and $\Delta T = T_{200} - T_0$ is the temperature difference, is a natural criterion or method for comparing observational and simulation data.

6. SIMULATION OF THERMAL STRATIFICATION IN NUMERICAL MODELS AND ITS DIFFERENCE BETWEEN THE URBAN AND RURAL LOCALITIES

As an example, we have chosen October 2018 to compare differences in thermal stratification under different meteorological conditions and at different points, demonstrate the features of the heat island dynamics and the simulation of thermal stratification in models, and more clearly show differences associated with clear and cloudy weather conditions.

Figure 5a shows the temporal variations in thermal stratification according to measurements in the urban environment. It is clearly seen that the differences in thermal stratification between urban and rural localities (see Fig. 4b) are especially pronounced under clear weather conditions and strong diurnal variations in the radiation balance. Note that comparing the time series of stratification for the summer and winter months over a few years of observations (see also Fig. 6) adds considerable support for this conclusion, although it is also supported by results of many other comparisons [11, 12]. However, in the numerical models, as is seen in Figs. 5b and 5c, the difference in thermal stratification throughout the ABL is almost unnoticeable.

This difference in thermal stratification in the lower part of the ABL between the urban and rural localities (compare Figs. 4 and 5) should differ by about a factor of two under maximum stability: if stable stratification with a gradient of 4°C/100 m is forecasted for the rural locality, then it will be about 2ºC/100 m for the urban locality. So far, according to model data, the difference in temperature gradients between the urban and rural localities amounts to 10−
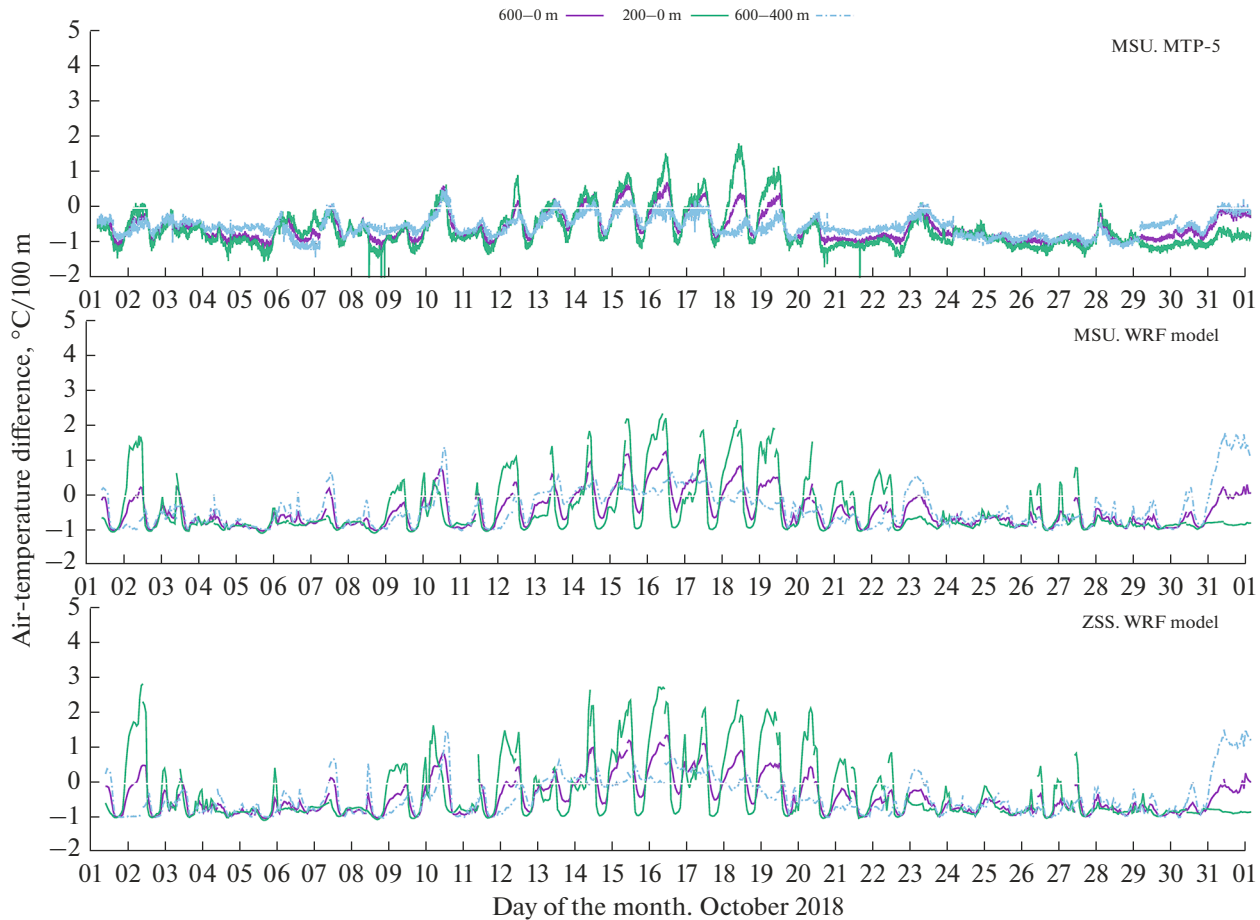
Fig. 5. Temporal variations in the air-temperature difference (similarly to Fig. 4b) for the urban (MSU) locality and according to numerical simulation at the two points. October 2018.

15% and may be lost against the background of forecast errors.

Of course, differences in temporal variations of thermal stratification between the urban and rural localities should be adequately described by models. However, if there is no possibility to correct models, these systematic forecast errors may be corrected. In addition, if the errors in the model ABL temperature fields depend on stratification values or the Richardson number, the construction of empirical correcting tables or their approximating empirical functions may be helpful.

On the whole, one can arrive at two conclusions. First, improved numerical models and urban ABL parameterizations may be compared based on their efficiency in describing ABL thermal-stratification variations for both urban and rural localities. In addition, second, estimating the ABL thermal-stratification variations through the difference between average vertical temperature gradients is a simple and convenient tool for measuring the urban heat island intensity that is less sensitive to spatial temperature-field inhomogeneities of a synoptical scale.

7. COMPARISON OF MEASURED BRIGHTNESS TEMPERATURES AND THE POSSIBILITY OF USING AN "OBSERVATION OPERATOR"

As was noted, the method of retrieving temperature profiles using a scanning microwave radiometer assumes that the medium under study has a layered homogeneity, which is naturally violated in urban canyons [12]. Moreover, there were doubts concerning the possible role of errors associated with absolute temperature measured by an external monitor sensor, the local overheating of which at the measurement point results in a shift of the entire profile, and heating from the building (on which the observation instruments are installed) at night could hypothetically change the temperature profiles. Therefore, the conclusions were checked using indirect methods.

The data on brightness temperatures directly measured by a radiometer at different angles are free of errors in retrieving temperature profiles. In other words, comparing brightness contrasts measured at the zenith, the horizon, and from other angles with the same differences measured within both urban and rural localities or at different points of the urban envi-
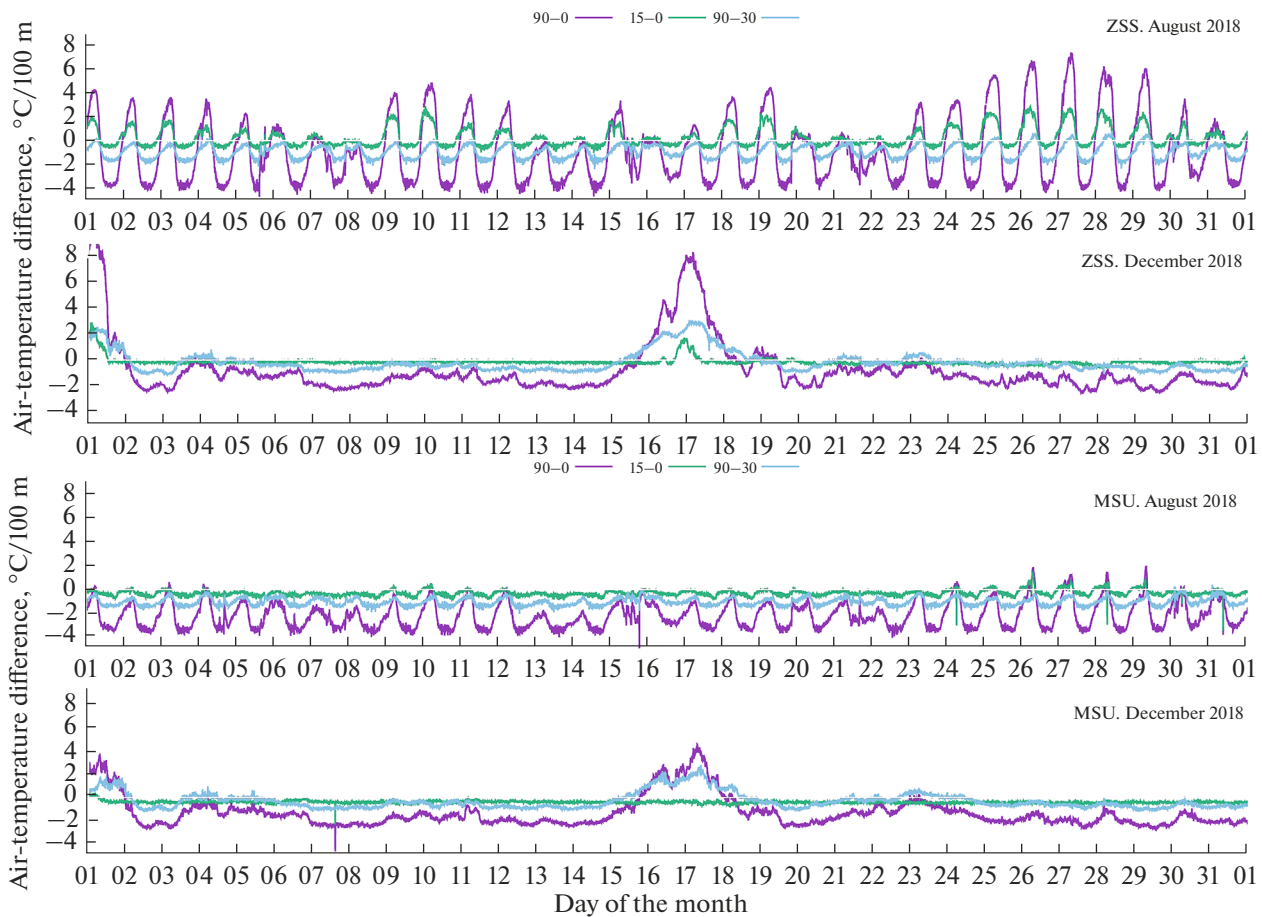
Fig. 6. Temporal variations in the difference between brightness temperatures measured by a microwave profiler at different angles in the rural (ZSS, top) and urban (MSU, bottom) localities in winter and summer as an example of brightness contrasts and the sensitivity of the measurements to thermal-stratification variations.

ronment gives one confidence in the significance of measured differences, but does not allow one to directly estimate thermal stratification variations.

The brightness temperature contrasts measured at angles of 90° (zenith), 0° (horizon), 90°−30°, and 15°−0° are compared in Fig. 6. The comparison of the two latter differences shows to what extent the difference in brightness temperatures at small elevations contributes to the general contrast, or how much variations in stable stratification in the lower part of the ABL within the urban environment affect the general temperature contrast.

It is seen that ABL temperature stratification variations are clearly observed under inversions: at night in summer and under anticyclonic conditions and radiation cooling of the surface in winter. In other words, the radiometric measurements of the urban heat island are very reliable and may serve a basis for tuning models and ABL parameterizations.

In recent decades, assimilation of remote sensing data has passed from the conventional methods of assimilating errors in calculated fields to the assimilation of the integral characteristics of these fields directly mea-

sured by remote sensing instruments from satellites and from the surface. To this end, the formal concept of an "observation operator", which characterizes the integrating properties of measuring instruments, is introduced. In this connection, the brightness temperature contrasts, which may be obtained from both model temperature and pressure fields through the solution of the direct problem of propagation of microwave radiation in the ABL, provide one more convenient tool for comparing different ABL parameterizations.

8. LOCAL VARIATIONS AND COMMON TEMPERATURE-GRADIENT FEATURES ACCORDING TO MEASUREMENTS AT DIFFERENT URBAN AND RURAL SITES

One complicated problem in carrying out high-technology and technically expensive measurements is the problem of the possibility of generalizing data obtained from measurements at a concrete observation point, the ABL characteristics of the metropolis as a whole, and common features of those properties that were found from measurements at two points. The local
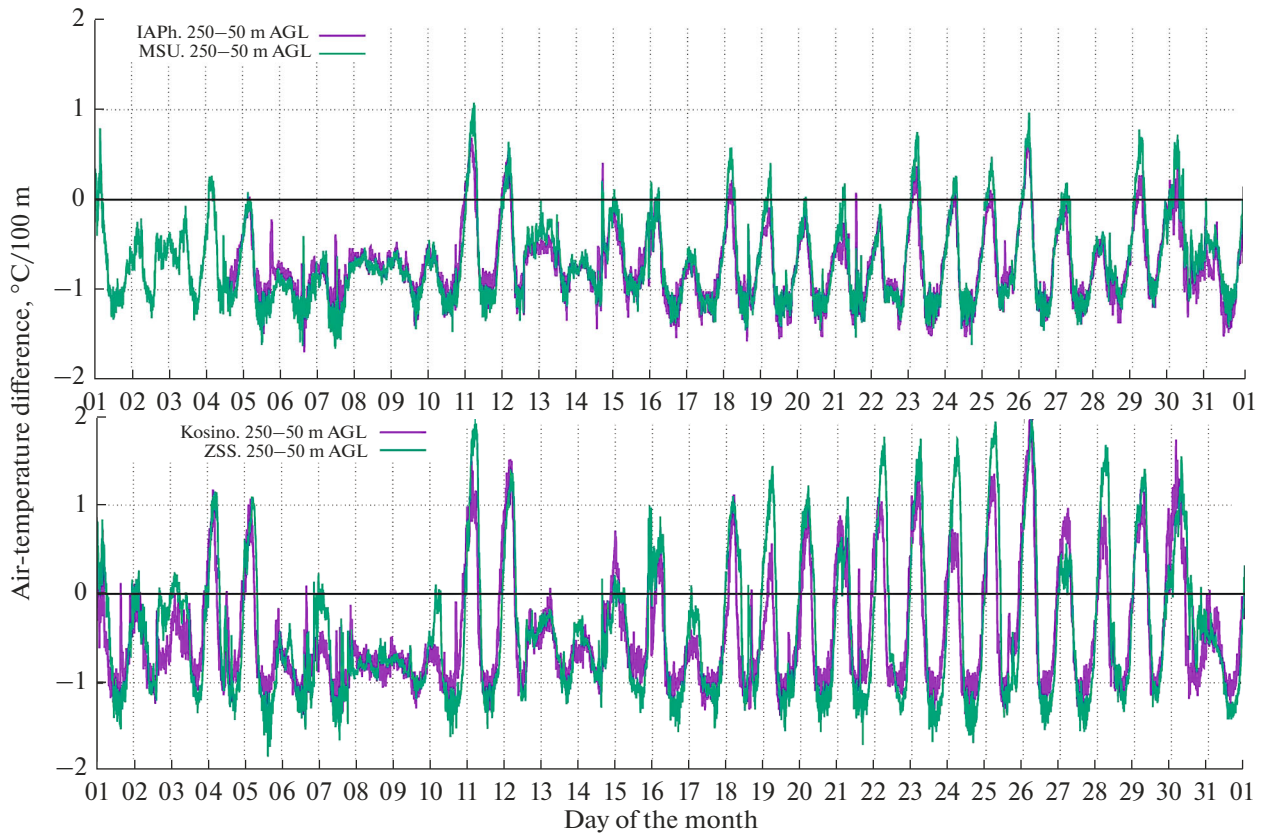
Fig. 7. Comparison of measurement data on average vertical temperature gradients (250–50 m) at the points of the urban (MSU and IAPh) and rural (ZSS and Kosino) localities. July 2017.

features of measurements carried out at urban meteorological stations within the atmospheric near-surface layer are well known [35, 36]. For example, for Moscow, the local features of meteorological measurements are especially noticeable at the Balchug station located in the center of the capital [37]. Therefore, the remote measurements of temperature fields over the city using several instruments installed at different points and operating for a sufficiently long time (for a year or more) yield reliable information on the spatial inhomogeneity of the urban heat island and its mean amplitude.

For such a comparison, we have chosen July 2017 and used measurement data obtained at the IAPh and the MEM network. High diurnal contrasts in summer and comparisons of temperature differences in the lower part of the ABL provide an estimate of the reliability of radiometric measurements and the repeatability (homogeneity) of thermal stratification properties within the urban environment.

The results of measurements performed at the IAPh (in the center of Moscow), at MSU (Vorob'evy Gory), at the ZSS (Zvenigorod), and in the Kosino district (combustion plant no. 4) outside the urban environment are compared in Fig. 7. These joint measurements show that the thermal stratification within the urban environment differs significantly from that in the rural locality during the night radiation cooling

and differs slightly during convective mixing. During the daylight hours, the vertical convective mixing is combined with the horizontal (advective) transport, which reduces spatial temperature contrasts.

It is seen that the properties of thermal stratification in the urban environment are clearly pronounced even despite the facts that at different measurement points the instruments of different modifications were used, these instruments were installed at different heights AGL, and the monitoring temperature sensors could response differently to the influence of buildings and constructions on which they are installed. Within the rural locality, the behavior of thermal stratification is almost the same despite a significant distance between the measurement points: Zvenigorod (50 km to the west of Moscow) and Kosino (eastern outskirts of the Moscow metropolis).

There is another conclusion, which should be emphasized. The numerical models in their parameterizations sharply restrict convective mesoscale variations in thermal stratification (see Figs. 5b, 5c); i.e., they do not allow spatial inhomogeneities and convective instabilities to develop, including in the urban environment. This, in its turn, leads to underestimation of turbulent exchange and mesoscale circulation and, for example, at low wind velocities, to an excessive accumulation of pollutants in the air basin of the

metropolis according to model calculations, which, however, is not observed in reality [38]. Of course, this does not suggest that the Moscow air basin is clear, but characterizes systematic errors in the numerical simulation of the transport of atmospheric pollutants. In addition, the systematic errors (see Fig. 3) in forecasting temperature fields near the surface are clearly indicative of this.

9. CONCLUSIONS

The analysis performed showed that the MTP-5 scanning temperature microwave radiometers operating within a band of 60 GHz are a reliable tool for measuring average thermal stratification in the ABL. The network of such radiometers in Moscow oblast demonstrates their long-term synchronous operation within both urban and rural localities. These radiometers may become a simple and reliable tool for estimating ABL parameterizations in numerical urban-environment models with a high spatial resolution.

Temporal variations in the ABL thermal stratification have a good property: they are, to a large extent, stationary, and synoptical conditions change mainly the amplitude of its diurnal variations. This property makes it possible to compare temporal variations at different observation points and different heights, and, using this parameter, one can compare different model parameterizations.

The comparison of temporal ABL thermal stratification variations obtained with the WRF mesoscale model and from radiometric measurements within the Moscow metropolis and its outskirts shows that the detailed mesoscale models of the WRF type, on the whole, adequately simulate diurnal variations in the ABL thermal stratification, and stratification changes caused by the influence of the urban environment are almost unnoticeable in current models, as opposed to microwave measurement data, which show significant differences in thermal stratification at different points of the metropolis.

The systematic error of the numerical mesoscale models lies in the simulation of significant temperature inversions in the urban environment at night in winter, when they are absent in measurement data. Such errors may be associated with inaccurate calculations of the ABL radiation balance under continuous stratus clouds. Under unstable stratification, including winter, the models too rapidly dampen instabilities occurring at temperature gradients that are larger than the adiabatic one, which results in underestimation of these gradients and their dynamics in the lower part of the ABL (0−200 m) in the models.

A simple algorithm for estimating numerical errors in the models as a difference between ultra-short-term (3 h) and diurnal (27 h) forecasts has been proposed. The statistical estimate of these errors shows that, for both urban and rural localities, they almost do not differ in the models but they are systematically signifi-

cant, namely, in the vicinity of the surface, especially in summer. In other words, errors in forecasting surface air temperatures are associated, to a large extent, with the simulation of mixing processes in the ABL.

CONFLICT OF INTEREST

The author declares that he has no conflict of interest.

REFERENCES

1. https://www.mmm.ucar.edu/weather-research-and-forecasting-model.

2. https://www.cosmo-model.org.

3. https://code.mpimet.mpg.de/projects/iconpublic.

4. X. Wen, S. Lu, and J. Jin, "Integrating remote sensing data with WRF for improved simulations of oasis effects on local weather processes over an arid region in northwestern China," J. Hydrometeorol. **13** (2), 573−587 (2012).
https://doi.org/10.1175/JHM-D-10-05001.1

5. C. Zhang, Y. Wang, and K. Hamilton, "Improved representation of boundary layer clouds over the southeast Pacific in ARW-WRF using a modified Tiedtke cumulus parameterization scheme," Mon. Weather Rev. **139** (11), 3489−3513 (2011).
https://doi.org/10.1175/MWR-D-10-05091.1

6. N. A. Kalinin, A. N. Shikhov, and A. V. Bykov, "Forecasting mesoscale convective systems in the Urals using the WRF model and remote sensing data," Russ. Meteorol. Hydrol. **42** (1), 9−18 (2017).
https://doi.org/10.3103/S1068373917010022

7. A. S. Monin and A. M. Yaglom, *Statistical Fluid Mechanics*, Vols. 1−2 (Nauka, Moscow, 1965−1967) [In Russian].

8. H. E. Landsberg, *The Urban Climate* (Academic Press, 1981).

9. *Urban Air Pollution in Megacities of the World* (Blackwell Publishers, Oxford, UK, 1992).

10. T. R. Oke, "The energetic basis of the urban heat island," Quart. J. R. Meteorol. Soc. **108** (455), 1−24 (1982).
https://doi.org/10.1002/qj.49710845502

11. R. B. Stull, *An Introduction to Boundary Layer Meteorology* (Springer, 1988).

12. A. J. Arnfield, "Two decades of urban climate research: A review of turbulence, exchanges of energy and water, and the urban heat island," Int. J. Climatol. **23** (1), 1−26 (2003).
https://doi.org/10.1002/joc.859

13. J. A. Voogt and T. R. Oke, "Thermal remote sensing of urban climates," Remote Sens. Environ. **86** (3), 370–384 (2003).
https://doi.org/10.1016/S0034-4257(03)00079-8

14. N. Schwarz, U. Schlink, U. Franck, and K. Großmann, "Relationship of land surface and air temperatures and its implications for quantifying urban heat island indicators—An application for the city of Leipzig (Germany)," Ecol. Indic. **18**, 693–704 (2012).
https://doi.org/10.1016/j.ecolind.2012.01.001

15. A. Derdouri, R. Wang, Y. Murayama, and T. Osaragi, "Understanding the links between LULC changes and SUHI in cities: Insights from two-decadal studies (2001–2020)," Remote Sens. **13** (18), 3654 (2021).
https://doi.org/10.3390/rs13183654

16. A. Rasul, H. Balzter, C. Smith, et al., "A review on remote sensing of urban heat and cool islands," Land **6** (2), 38 (2017).
https://doi.org/10.3390/land6020038

17. B. Schonwald, "Determination of vertical temperature profiles for the atmospheric boundary layer by ground-based microwave radiometry," Boundary-Layer Meteorol. **15** (4), 453–464 (1978).
https://doi.org/10.1007/BF00120607

18. K. P. Gaikovich, E. N. Kadygrov, A. S. Kosov, and A. V. Troitskii, "Thermal sounding of the atmospheric boundary layer in the center of an oxygen absorption line," Radiophys. Quantum Electron. **35** (2), 93–97 (1992).

19. E. N. Kadygrov, I. N. Kuznetsova, and G. S. Golitsyn, "Heat island in the boundary atmospheric layer over a large city: New results based on remote sensing data," Dokl. Akad. Nauk. **385** (2), 688–694 (2002).

20. U. Löhnert, S. Crewell, O. Krasnov, et al. "Advances in continuously profiling the thermodynamic state of the boundary layer: Integration of measurements and methods," J. Atmos. Ocean. Technol. **25** (8), 1251–1266 (2008).
https://doi.org/10.1175/2007JTECHA961.1

21. V. P. Yushkov, "What can be measured by the temperature profiler?," Russ. Meteorol. Hydrol. **39** (12), 838–846 (2014).
https://doi.org/10.3103/S1068373914120097

22. M. M. Smirnova, K. G. Rubinshtein, and V. P. Yushkov, "Evaluation of atmospheric boundary layer characteristics simulated by the regional model," Russ. Meteorol. Hydrol. **36** (12), 777–785 (2011).
https://doi.org/10.3103/S1068373911120016

23. J. Michalakes, J. Dudhia, D. Gill, et al., "The weather research and forecast model: Software architecture and performance," in *Proceedings of the Eleventh ECMWF Workshop on the Use of High Performance Computing in Meteorology* (World Scientific, Singapore, 2005), pp. 156–168.
https://doi.org/10.1142/9789812701831_0012.

24. W. C. Skamarock, J. B. Klemp, J. Dudhia, et al., *Description of the Advanced Research WRF Version 3* (University Corporation for Atmospheric Research, 2008), NCAR Technical Note NCAR/TN-475+STR.
https://doi.org/10.5065/D68S4MVH

25. https://www.emc.ncep.noaa.gov/emc/pages/numerical_forecast_systems/gfs/documentation.php.

26. G. Thompson, R. M. Rasmussen, and K. Manning, "Explicit forecasts of winter precipitation using an improved bulk microphysics scheme. Part I: Description and sensitivity analysis," Mon. Weather Rev. **132**, 519–542 (2004).
https://doi.org/10.1175/1520-0493(2004)132<0519:EFOWPU>2.0.CO;2

27. M. J. Iacono, J. S. Delamere, E. J. Mlawer, et al., "Radiative forcing by long-lived greenhouse gases: Calculations with the AER radiative transfer models," J. Geophys. Res. **113**, D13103 (2008).
https://doi.org/10.1029/2008JD009944

28. M. B. Ek, K. E. Mitchell, Y. Lin, et al., "Implementation of Noah land surface model advances in the National Centers for Environmental Prediction operational mesoscale Eta model," J. Geophys. Res.: Atmos., **108**, D22 (2003).
https://doi.org/10.1029/2002JD003296

29. G. A. Grell and D. Devenyi, "A generalized approach to parameterizing convection combining ensemble and data assimilation techniques," Geophys. Res. Lett., **29**, 1693 (2002).
https://doi.org/10.1029/2002GL015311

30. P. Bougeault and P. Lacarrere, "Parameterization of orography-induced turbulence in a mesobeta-scale model," Mon. Weather Rev. **117**, 1872–1890 (1989).
https://doi.org/10.1175/15200493(1989)117<1872:POOITI>2.0.CO;2

31. J. W. Deardorff, "Theoretical expression for the countergradient vertical heat flux," J. Geophys. Res. **77** (30), 5900–5904 (1972).
https://doi.org/10.1029/JC077i030p05900

32. F. Chen, H. Kusaka, R. Bornstein, et al., "The Integrated WRF/urban modelling system: Development, evaluation, and applications to urban environmental problems," Int. J. Climatol. **31** (2), 273–288 (2011).
https://doi.org/10.1002/joc.2158

33. V. P. Yushkov, M. M. Kurbatova, M. I. Varentsov, et al., "Modeling an urban heat island during extreme frost in Moscow in January 2017," Izv., Atmos. Ocean. Phys. **55** (5), 389–406 (2019).
https://doi.org/10.1134/S0001433819050128

34. A. V. Troitsky, K. P. Gajkovich, V. D. Gromov, E. N. Kadygrov, and A. S. Kosov, "Thermal sounding of the atmospheric boundary layer in the oxygen absorption band center at 60 GHz," IEEE Trans. Geosci. Remote Sens. **31** (1), 116–120 (1993).
https://doi.org/10.1109/36.210451

35. H. E. Landsberg, "Meteorological observations in urban areas," in *Meteorological Observations and Instrumentation* (American Meteorological Society, Boston, Mass., 1970), pp. 91–99.
https://doi.org/10.1007/978-1-935704-35-5_14.

36. T. R. Oke, "Siting and exposure of meteorological instruments at urban sites," in *Air Pollution Modeling and Its Application XVII* (Springer, Boston, Mass., 2007), pp. 615–631.
https://doi.org/10.1007/978-0-387-68854-1_66.

37. M. A. Lokoshchenko, "Urban 'heat island' in Moscow," Urban Clim. **10**, 550–562 (2014).
https://doi.org/10.1016/j.uclim.2014.01.008

38. N. Ponomarev, V. Yushkov, and N. Elansky, "Air pollution in Moscow megacity: Data fusion of the chemical transport model and observational network," Atmosphere **12** (3), 374 (2021).
https://doi.org/10.3390/atmos12030374

Translated by B. Dribinskaya